Analysis of Standing Droplets in Rat Proximal Tubules

R. R. WARNER and C. LECHENE

From the National Biotechnology Resource in Electron Probe Microanalysis, Harvard Medical School, Boston, Massachusetts 02115

ABSTRACT Volume, osmolality, and concentrations for Na, Cl, and raffinose have been measured as a function of time in standing droplets within rat intermediate and late proximal tubules. Standing droplet reabsorption proceeds without the development of a measurable osmotic difference across the epithelium. After 140 s of tubular exposure, droplet-to-plasma concentration differences are observed for raffinose, Na, and Cl with the observed Na concentration difference, usually referred to as limiting gradient, being ~9 mM. It is possible that a smaller or even no limiting difference would be attained with longer exposure times. Previous values measured for the limiting Na concentration in the rat proximal tubule were determined before the attainment of constant concentrations. Assuming that the Na concentration we measured is the limiting value, we estimate that active NaCl transport accounts for a very small fraction, <6%, of the volume reabsorption; using an alternative approach of fitting a theoretical model to our experimental data, active NaCl transport is again estimated to account for only 6% of the total reabsorbate. The previous interpretation that a limiting Na concentration gradient constitutes the most direct evidence for active Na transport may be in error; the gradient we measure can be modeled without incorporating active NaCl transport.

INTRODUCTION

It is generally accepted that in the proximal tubule a large fraction of the filtered load is actively reabsorbed and that active Na transport is the major driving force for fluid reabsorption. These two ideas, however, can be questioned. One of the principal and most direct arguments for demonstrating active transepithelial Na transport in the proximal tubule (5, 8, 15, 23, 63–65) is the observation of a "limiting Na concentration gradient"* in standing droplets containing a poorly permeant solute (9, 11, 14, 20, 22, 24, 32, 35, 39, 62). The measurement of this gradient has even been used to calculate the

Address reprint requests to Dr. C. Lechene, Harvard Medical School, National Biotechnology Resource in Electron Probe Microanalysis, 221 Longwood Ave., Boston, Mass. 02115. Dr. Warner's present address is Procter and Gamble Co., Miami Valley Laboratories, Cincinnati, Ohio 45247.

* To conform with previous literature, we will use here the word "gradient." The word "difference," however, would be more correct.

J. GEN. PHYSIOL. © The Rockefeller University Press · 0022-1295/82/04/0709/27 $1.00 709
Volume 79 April 1982 709–735

apparent electromotive force of the active Na pump (16). Nevertheless, the interpretation that the limiting Na concentration gradient provides direct evidence for an active transepithelial Na pump is questionable, as is the very existence of a limiting Na concentration gradient (59, 60). Previous investigations of a limiting Na concentration gradient using high-molecular weight solutes, in which the partial molar solute volume is large, have not addressed problems of non-ideal solutions and have not applied a volume correction for water content (11, 59). Previous investigations using more permeant solutes such as raffinose may have measured droplet concentrations before the attainment of constant values (59, 60); limiting droplet concentrations were initially reported to be attained by 60 s (24), but there is no evidence that demonstrates the achievement of an invariant Na concentration by this time. Similarly, using a so-called "equilibrium solution" (Na concentration identical to Na "limiting concentration value") as a tubular perfusate, net entry of Na has nevertheless been observed (38, 52), which suggests that measured standing droplet Na concentrations were not true "limiting" values.

If a steady state limiting Na concentration gradient does exist, it may not necessarily indicate the presence of an active Na transport pump (60). Poorly permeant solutes diffuse from the droplet, which complicates any intuitive understanding of droplet behavior (46, 60). The assumption that a limiting concentration gradient for an ion is due to the presence of an active pump neglects the effect of osmotic pressure of the poorly permeant solute, Donnan distributions, and electrical forces. Recent theoretical work on standing droplets from our laboratory (60), incorporating the osmotic force of solute asymmetry and the permeability of the poorly permeant solute, indicates that a limiting gradient could be obtained in the absence of active reabsorption.

The direct contribution of active transepithelial sodium transport in the proximal tubule to volume reabsorption may be minor. A substantial fraction of volume reabsorption may be due to the passive movement of salt, as has recently been suggested (11, 41, 42, 44, 57).

The present article describes experiments and theoretical analyses on the behavior of standing droplets containing raffinose in the rat intermediate and late proximal tubule. We have investigated the existence of a limiting Na concentration gradient and we have estimated the fraction of the volume reabsorption that is due to an active NaCl component. Droplet concentrations were measured using electron probe microanalysis, which permitted simultaneous analysis for Na, Cl, and raffinose in single very small droplet volumes at times up to 140 s. We found that a limiting Na concentration is not reached by 60 s. If a limiting Na concentration gradient is attained, this gradient is small and could be explained entirely by passive forces. Assuming the existence of a limiting concentration gradient, we calculate that active Na transepithelial transport cannot account for >6% of the reabsorbate. Using a different approach of fitting a theoretical model to our experimental data, active transepithelial NaCl transport was again estimated to account for ~6% of the volume reabsorption. The major fraction of volume flow is due to the passive forces of solute asymmetry and solvent drag.

METHODS

Preparation of Animals

Charles River female Wistar rats, 176–254 g, were fasted overnight and given Inactin at 148 mg/kg body wt. Animals were prepared for micropuncture as previously described (27). Isotonic saline was infused via the jugular vein at 5.8 ml/h; temperature was maintained between 37 and 38°C; blood was sampled from the femoral artery. The left kidney was mounted and immobilized in a cup, and the surface was bathed with paraffin oil warmed to 38°C. The kidney capsule was left intact.

Experiments were conducted on 63 rats. Investigations using an isotonic raffinose solution were conducted on 23 rats. Investigations using an equilibrium solution were conducted on 29 rats. Investigations using a nutrient solution were conducted on five rats. Osmolality measurements were performed on six rats.

Standing Droplet Technique

Single-barrelled sharpened glass micropipettes with tip diameters of 5–8 μm were used for droplet injection and collection. The micropipettes were siliconized with SC 87 (now Surfasil, Pierce Chemical Co., Rockford, Ill.) and prefilled with two 198-pl droplets of the appropriate test solution; the droplets were isolated from each other and from exposure to air by water-saturated unstained paraffin oil. Small volumes (198 pl) were used in order to maintain visual control of the droplets. Occasionally droplet volumes of 500 pl were used to obtain volumes large enough to be manipulated after long exposure times when using the equilibrium or nutrient solutions. The pipettes were stored in a water-saturated atmosphere until subsequent use that day.

For visibility, micropuncture was performed exclusively in the midregion of long surface segments of proximal tubules. It is unlikely that micropuncture occurred within the first 1 mm of the proximal tubule. After micropuncture, a small amount of oil was injected into the proximal tubular lumen to determine the direction of flow. In general, proximal tubules were selected for experimentation when the micropipette had entered the tubule with the orifice directed upstream. A large block of oil was then injected, followed by the first droplet. This droplet served to rinse the tubular lumen, minimizing contamination of the subsequent droplet with tubular fluid not displaced by the oil (31) and minimizing possible contamination incurred while puncturing the tubule. The first droplet was discarded by further oil injection. The second droplet of test solution was injected and isolated upstream from the injection site with additional oil. Position was maintained with further oil injection as required. After the appropriate tubular exposure time, the droplet was withdrawn into the same micropipette and isolated with oil from the tubular lumen. After collection, the droplet was immediately prepared for electron probe analysis. Approximately 10 droplets were obtained from each rat. Plasma was collected at the middle and end of the experiment.

Measurement of Droplet Volume and Ion Concentrations

Plasma ultrafiltrates and droplets were processed immediately after collection to avoid concentrating effects. The droplet volume was measured using calibrated volumetric micropipettes (29). Concentrations for Na, K, Ca, Mg, Cl, PO_4 (measured as P), and SO_4 (measured as S) were simultaneously determined in aliquots (usually 20–40 pl) of both ultrafiltrates and proximal tubular droplets by electron probe microanalysis using the liquid droplet technique (28, 29). All samples were analyzed in triplicate whenever possible, standards were run in quintuplicate. Analysis was performed with

an automated (37) Cameca MS46 microprobe (Cameca Inc., Stamford, Conn.) operated at 11 kV and 200 nA sample current (measured on Be); the beam diameter was usually 60–80 μm. Na and Mg were analyzed with a potassium acid phthalate crystal. K, Ca, Cl, P, and S were analyzed with a pentaerythritol crystal. Data were reduced using a Hewlett-Packard 2100 minicomputer (Hewlett-Packard Co., Palo Alto, Calif.) (37).

Measurement of Raffinose Concentration

Droplet raffinose concentrations were determined by electron probe microanalysis. Raffinose concentrations were measured in the same samples as the other seven physiological elements, using a lead stearate crystal to measure characteristic carbon x-rays. This procedure is justified because raffinose is the predominant carbon-containing substance present in the standing droplet, and would probably contain more carbon than any organic acid that could be secreted even at equal osmolarity. The carbon x-ray counts of the unknown were compared with the carbon x-ray counts of the standards, made of raffinose solutions of known concentration. Over the raffinose concentration range used, 0–300 mM, the carbon x-ray counts were linearly related to the raffinose concentration (Fig. 1). Standards, samples, and background were counted for identical times to compensate for carbon contamination in the electron probe.

Test Solutions

Three separate test solutions were used. They were prepared anew in general after 2 wk and did not contain dyes. The raffinose solution was an isotonic solution of raffinose (Eastman Organic Chemicals, Eastman Kodak Co., Rochester, N. Y.) with an average osmolality of 300 ± 7 mosmol/kg (n = 5). The equilibrium solution composition was selected to resemble the so-called "equilibrium" concentrations

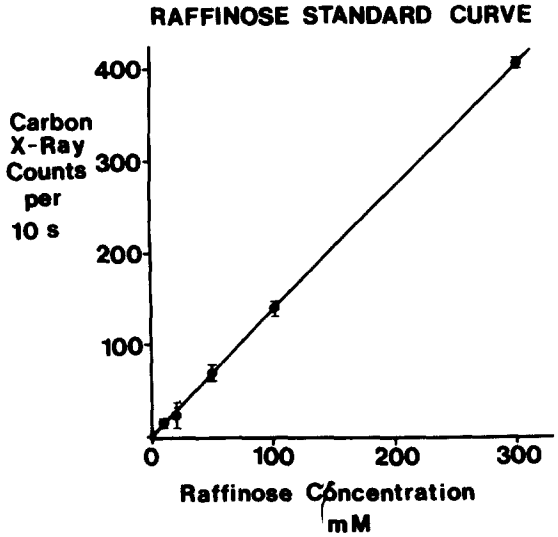

FIGURE 1. Correlation between raffinose concentration and carbon K x-ray counts. Correlation coefficient is 0.9999. Droplet volume was 32 pl. Each point is the mean count from five aliquots. Error bars are standard deviations.

previously obtained in standing droplet experiments for Na, Cl, K, and Ca (9, 11, 20, 22, 24, 25, 32, 33, 35, 39, 52, 56), and plasma ultrafiltrate values for Mg, PO_4, and SO_4 (1). The average osmolality was 295 ± 4 mosmol/kg (n = 6). The nutrient solution was similar to the equilibrium solution except that $NaHCO_3$, glucose, and alanine replaced a fraction of the NaCl and raffinose. Composition of the test solution was measured in droplets from prefilled micropipettes selected at random, one before and one after the micropuncture experiment. Results for the three test solutions are reported in Table I.

Measurement of Osmolality

In six separate experiments using the isotonic raffinose solution, osmolality of the collected droplets and whole plasma was measured using freezing point depression according to the procedure of Ramsay and Brown (43). A collected droplet or standard was placed under oil, an aliquot was obtained with a volumetric micropi-

TABLE I
COMPOSITION OF TEST SOLUTIONS

	Raffinose solution	Equilibrium solution	Nutrient solution
	mM	*mM*	*mM*
Na	0.38±0.98	129±2.3	121±0.97
Cl	−0.48±1.16	132±3.0	95±4.1
K	0.11±0.06	4.07±0.15	3.21±0.13
Ca	0.25±0.06	1.49±0.08	1.05±0.17
Mg	−0.09±0.06	1.26±0.07	1.53±0.14
PO_4	0.68±0.11	2.08±0.08	1.29±0.09
SO_4	0.07±0.11	1.51±0.14	20*
HCO_3	—	—	5.0*
Acetate	—	5.0*	54±2.0
Raffinose	300*	59.2±4.0‡	5.0*
Glucose	—	—	5.0*
Alanine	—	—	n = 5
	n = 22	n = 29	

* Not measured.
‡ n = 10.

pette, and this aliquot was taken up in a micropuncture micropipette. The aliquot volume varied between 58 and 78 pl, but was constant during an experiment. The temperature endpoint, taken when the last crystal of ice disappeared, was measured directly from a thermometer (Brooklyn Thermometer Co., New York; +1 to −9°C). Droplet osmolality was measured immediately after collection from a proximal tubule. Standards of known osmolality were measured at the beginning and end of each series of measurements. Standards used were 0, 100, 290, and 500 mosmol/kg (Wescor Inc., Logan, Utah).

Plasma Ultrafiltration

Plasma was ultrafiltered under oil using single Amicon hollow dialysis fibers (P.M. 30; Amicon Corp., Lexington, Mass.). These fibers have an inner diameter of 0.2 mm and a molecular weight cutoff of 30,000. Before use they were rinsed and soaked in distilled water for 24 h, followed by 24 h of drying at 85°C. Plasma was drawn up the

hollow core of these fibers and the fibers were folded in half and placed within pulled, sealed, oil-filled capillary tubes. By centrifugation, plasma was filtered out of the fiber and collected at the bottom of the pulled capillary.

Droplet Conservation

Because of the small volumes used in these experiments, any loss of water to the surrounding oil could introduce systematic errors in the determination of droplet concentrations. To test this possibility, microliter droplets containing 100 mM NaCl were placed on a concavity slide under water-saturated oil; no detectable concentration changes occur in droplets this size over a period of several hours (30). From this source droplet, 198-pl aliquots were taken and placed on the surface of the same concavity slide; these droplets were immediately picked up individually in micropipettes, isolated by oil, and stored in a water-saturated atmosphere. At timed intervals, several of the stored droplets were expelled under oil and three aliquots of each were taken for microanalysis using the liquid droplet technique (28, 29). The composition of the stored droplets was compared with the composition of aliquots obtained directly from the source droplet (Fig. 2).

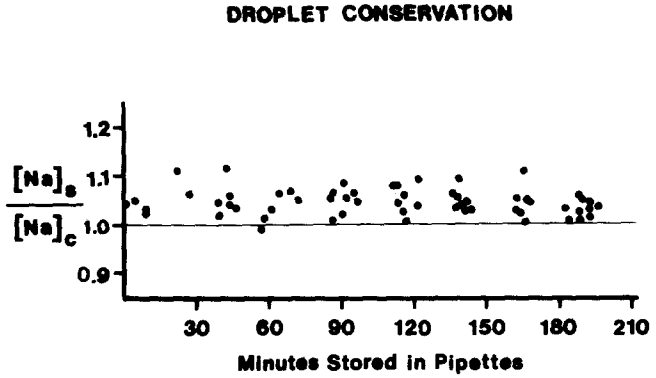

FIGURE 2. Na concentration from 198-pl aliquots of a 100-mM NaCl solution ($[Na]_s$) stored in micropipettes, compared as a function of time with the Na concentration of the same solution from a large volume kept under oil ($[Na]_c$). Each point represents a single droplet; determinations are from four separate experiments.

Statistics

All values reported are means with their standard errors, except as noted. A value of $P = 0.05$, determined using an unpaired t test, was the criterion for a statistically significant difference betweens means.

Theoretical Models

A theoretical expression for the magnitude of a limiting concentration gradient was derived from equations describing the movement of salt and raffinose in standing droplets (Appendix A). These equations include the major reabsorptive forces. The maximum contribution of active NaCl transport to volume reabsorption was evaluated from this expression for the limiting concentration gradient.

The contribution of active NaCl transport to volume reabsorption was also evalu-

ated by theoretically modeling the standing droplet experiment, solving the differential equations in closed form (Appendix B), and comparing the solution with our experimental data. By adjusting the contribution of active NaCl reabsorption in the theoretical model until a good fit was obtained with the experimental data, the fraction of total droplet reabsorption due to active NaCl reabsorption was estimated.

RESULTS

Glomerular Filtration Rate (GFR)

As a control of whole kidney function, GFR was measured in six rats and averaged 1.04 ± 0.07 ml/min.

Plasma Ultrafiltrate Concentrations

In animals studied by using the isotonic raffinose solution, average plasma ultrafiltrate concentrations were 147 ± 1 mM for Na and 112 ± 3 mM for Cl ($n = 23$). In animals studied by using the equilibrium solution, average plasma ultrafiltrate concentrations were 145 ± 1 mM for Na and 116 ± 3 mM for Cl ($n = 29$).

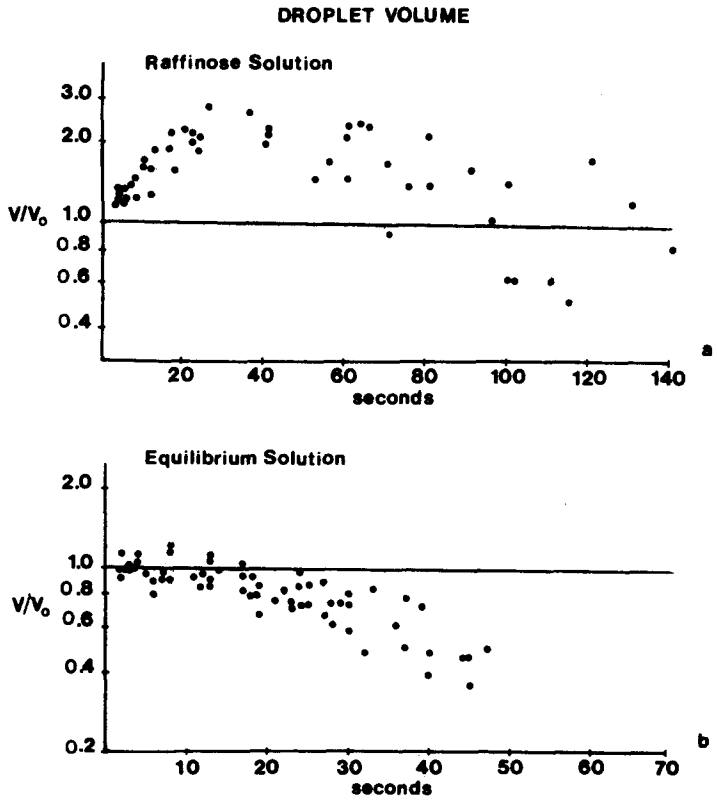

FIGURE 3. Droplet volume (V) as a function of tubular exposure time for the isotonic raffinose and equilibrium solutions. V_0 is the initial droplet volume (198 pl). Each point represents a single droplet.

Droplet Volume

The change in droplet volume with time is shown in Fig. 3. With the isotonic raffinose solution (Fig. 3*a*) the droplet first increases in volume before net reabsorption occurs. Droplet volume increases to a maximum of ~2.5 times the initial volume at times near 30 s.

With the equilibrium solution (Fig. 3*b*), droplet volume appears to decrease continuously, being relatively slow for ~10 s and somewhat more rapid thereafter.

Droplet Na and Cl Concentrations

The change in droplet Na and Cl concentrations with time are shown in Figs. 4 and 5 for the isotonic raffinose and equilibrium solutions, respectively. Na concentrations are at all times approximately identical to the Cl concentrations. With isotonic raffinose, Na and Cl rapidly enter the droplets (Fig. 4).

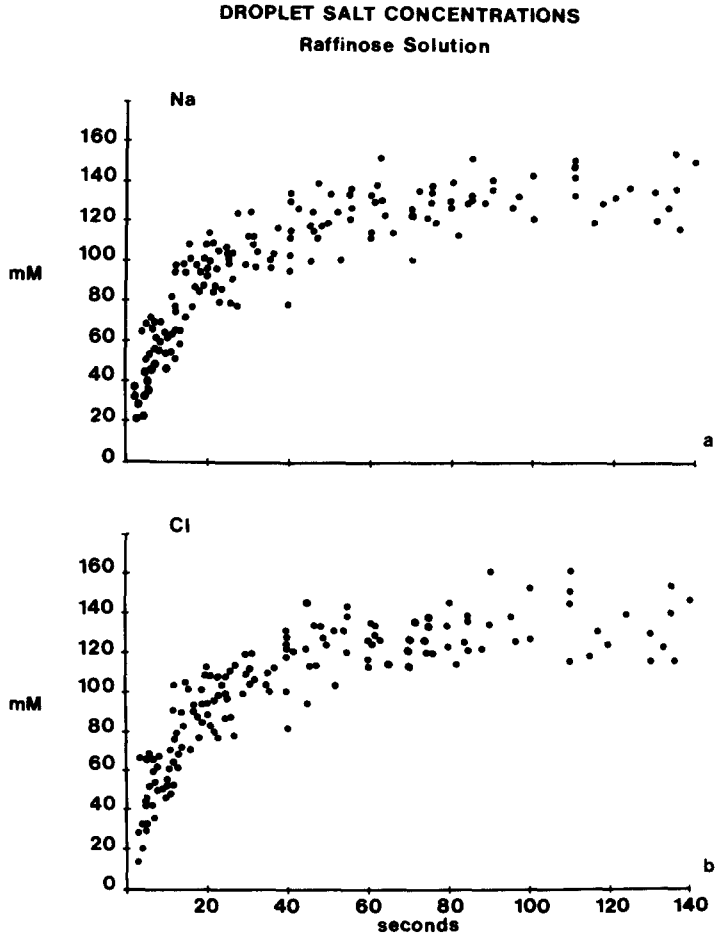

FIGURE 4. Droplet Na and Cl concentrations as a function of tubular exposure time using the isotonic raffinose solution. Each point represents a single droplet.

During droplet volume decrease (after 40 s; Fig. 3*a*), Na and Cl concentrations continue to increase at a slow rate (Table II). Between 50 and 70 s, the average Na concentration is 124 ± 3 mM and the average Cl concentration is 125 ± 2 mM (n = 19). Between 100 and 140 s, the average Na concentration is 135 ± 3 mM and the average Cl concentration is 134 ± 4 mM (n = 17). These latter values are significantly higher than those at the earlier time points (Table II).

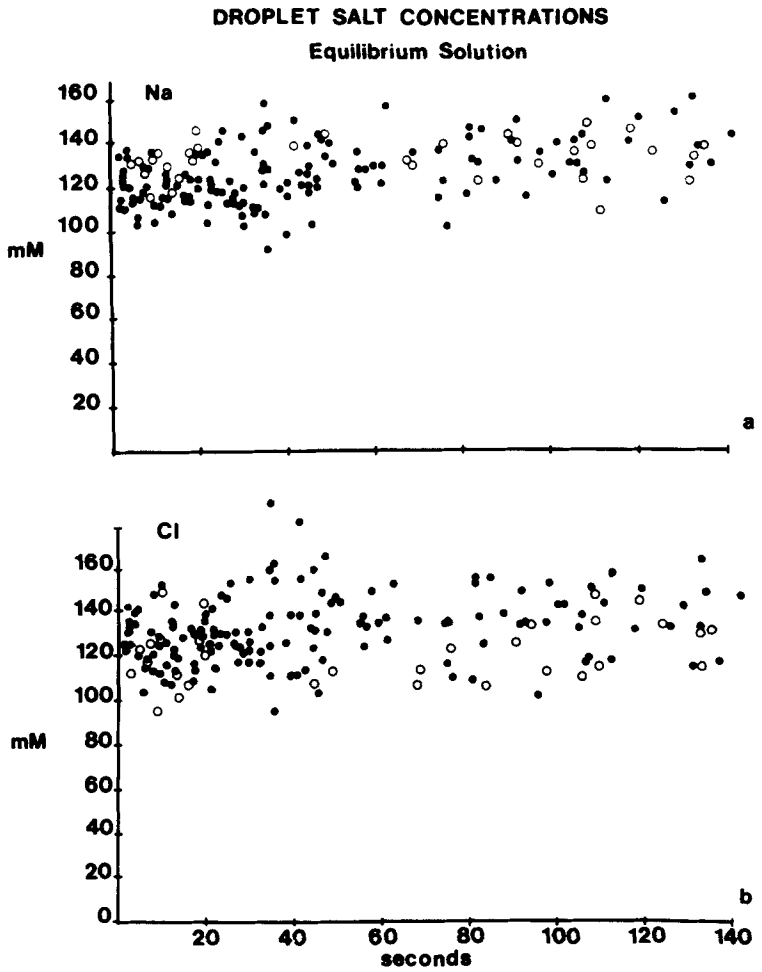

FIGURE 5. Droplet Na and Cl concentrations as a function of tubular exposure time using the equilibrium solution (closed circles) and the nutrient solution (open circles). Each point represents a single droplet.

With the equilibrium solution (Fig. 5), Na and Cl concentrations slowly increase with time during droplet volume decrease (cf. Fig. 3*b*). Between 10 and 25 s the average Na concentration is 123 ± 2 mM and the average Cl concentration is 125 ± 2 mM (n = 34). Between 100 and 141 s the average Na concentration is 137 ± 3 mM and the average Cl concentrations is 137 ± 3

mM (n = 19). These latter values are significantly higher than the earlier time points (Table II).

To test whether the droplet concentrations were affected by the omission of glucose, alanine, and HCO_3 from the initial droplet solution, experiments were repeated using the nutrient solution (Fig. 5). The mean droplet concentration between 100 and 140 is 133 ± 4 mM for Na and 128 ± 5 mM for Cl (n = 10); these values are not statistically different from those obtained with the equilibrium solution (P = 0.9 and P = 0.1, respectively). Therefore, the presence or absence of glucose, alanine, and HCO_3 appears to have no effect on droplet Na and Cl concentrations at long exposure times, and consequently the values from these two solutions have been pooled (between 100 and 140 s, Na = 136 ± 2 mM, Cl = 135 ± 3 mM; n = 29).

Droplet Raffinose Concentration

Fig. 6 shows the change in droplet raffinose concentration with time for the isotonic raffinose and equilibrium solutions. Using the isotonic raffinose solution (Fig. 6*a*), the raffinose concentration rapidly decreases because of dilution during the droplet volume increase (cf. Fig. 3*a*), and because of

TABLE II

STANDING DROPLET CONCENTRATIONS

Isotonic raffinose solution	50–70 s	100–140 s	P
	mM	*mM*	
Na	124±3 (19)*	135±3 (17)	<0.01
Cl	125±2 (19)	134±4 (17)	<0.05
Raffinose	41±2 (7)	33±2 (8)	<0.05
Equilibrium solution	**10–25 s**	**100–141 s**	P
Na	123±2 (34)	137±3 (19)	<0.01
Cl	125±2 (34)	137±3 (19)	<0.01
Raffinose	42±4 (13)	33±4 (19)	NS‡

* Number of observations.

‡ Not statistically significant at $P \leq 0.05$

diffusion out of the droplet. During droplet volume decrease (cf. Fig. 3*a*), the raffinose concentration slowly decreases. Raffinose concentrations obtained between 100 and 140 s are lower than those obtained between 50 and 70 s (Table II). Using the equilibrium solution (Fig. 6*b*), the raffinose concentration slowly decreases with time as the droplet volume decreases (cf. Fig. 3*b*); the concentration obtained between 0–10 s is significantly higher than that obtained between 100–140 s (P = 0.02), although the difference between the 10–25-s and 100–140-s intervals is not statistically significant because of the scatter of the data (Table II).

Maximum Limiting Concentration Gradients

If droplet Na and Cl concentrations measured between 100 and 140 s of tubular exposure represent reasonable *lower bounds* for the droplet limiting concentrations, then maximum limiting concentration gradients can be estimated. With the isotonic raffinose solution, the lower-limit Na concentration

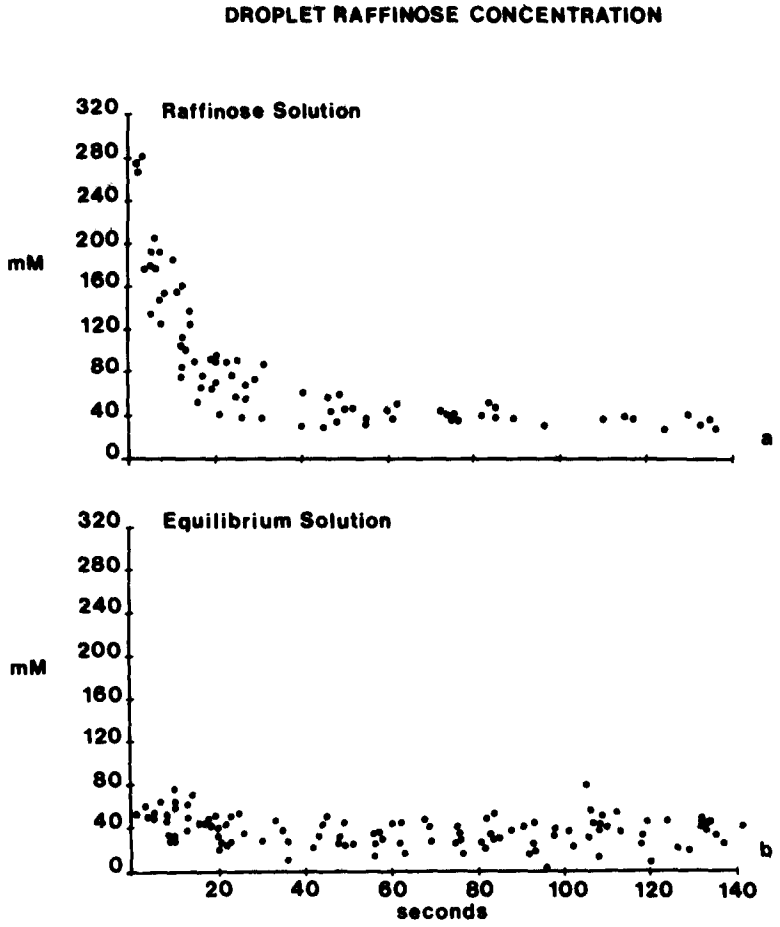

FIGURE 6. Droplet raffinose concentration as a function of tubular exposure time for the isotonic raffinose and equilibrium solutions. Each point represents a single droplet. Determinations were made in 11 rats with the isotonic raffinose solution and 16 rats with the equilibrium (and nutrient) solution.

of 135 mM ± 3 mM is significantly less than the plasma value ($P = 0.01$) with a maximum limiting Na concentration gradient of 12 ± 3 mM ($n = 17$). With the equilibrium solution, the lower-limit Na concentration of 136 ± 2 mM is signficantly less than the plasma value ($P = 0.02$) with a maximum limiting concentration gradient of 9 ± 2 mM ($n = 29$). With both solutions the droplet chloride concentration is significantly greater than the plasma chloride value ($P = 0.01$).

Droplet Osmolality

Freezing point depression measurements of standing droplet osmolality using the isotonic raffinose solution are shown in Fig. 7. The osmolality was invariant with time; the fitted least-square line had a correlation coefficient of 0.028, a slope (−0.0085 ± 0.0057) not statistically different from zero, and a mean

osmolality of 298 ± mosmol (n = 54). This mean value is not statistically different from the plasma osmolality of 302 ± 4.4 mosmol (n = 16 rats, P = 0.4).

DISCUSSION

Because only the midregions of long surface segments were micropunctured, the first 1 mm of the proximal tubule was likely to be excluded from these experiments. Consequently, our observations do not apply to this early region, which is morphologically and functionally distinct from the remaining intermediate and late proximal tubule (10, 12, 21, 36, 51).

If a good seal around the glass micropipette was not obtained, the droplet volume decreased extremely rapidly, which could even be observed during droplet ejection into the tubule. Contamination of droplet fluid by the

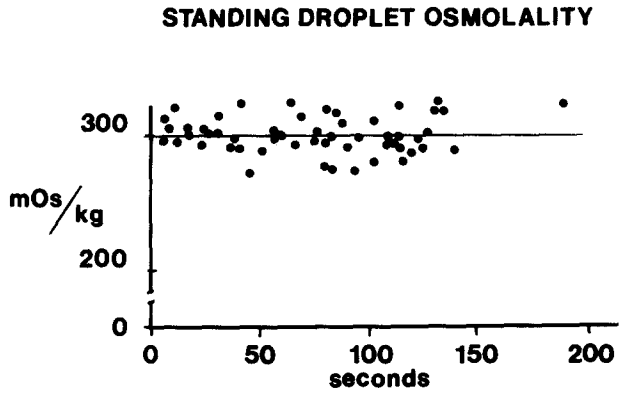

FIGURE 7. Droplet osmolality from freezing point depression measurements using the isotonic raffinose solution. Each point represents an individual droplet. The regression line was fitted by linear least squares; $y = -0.0085x + 297$(r = 0.028).

interstitium, adjacent tubules, or by leakage around the oil block was rare and readily detected by an abnormally large droplet volume with abnormal concentrations—in particular, an exceedingly low droplet raffinose concentration. The presence of cellular contamination was more frequently observed, with high values being obtained for droplet K and PO_4 concentrations. All questionable droplet collections were discarded; these constituted <15% of all micropunctures.

Droplet Volume

The standing droplet volume has previously been measured using photographic methods (13) or labeled (radioactive) non-reabsorbable markers (51). The latter procedure involves the inclusion of an additional poorly permeant solute in a droplet and would have introduced an additional complexity in these experiments. Our procedure of directly measuring the volume avoids some problems of the photographic technique (18, 19, 40) but introduces

other difficulties. The scatter in the droplet volume (Fig. 3) is probably due to errors involved in summed replicate measurements using one calibrated micropipette as well as difficulties in achieving complete droplet collection at long exposure times. With long exposure times the droplets often could not be prevented from moving downstream past the tip of the pipette, whereas reaspiration preferentially withdrew upstream contents. In spite of the different techniques used for volume measurement, the results with the isotonic raffinose solution are similar to previous measurements (13).

It is instructive to compare droplet volume (Fig. 3*a*) with droplet osmolality (Figs. 7*a* and 8) for the isotonic raffinose solution. During net reabsorption (after 40 s, cf. Fig. 3*a*), droplet osmolality appears to be equal to that of plasma, and reabsorption is consequently isotonic (58). However, at earlier times during net volume influx the droplet osmolality also appears to be equal to that of plasma, and net secretion appears to be isotonic. It is difficult to reconcile both isotonic reabsorption and secretion in the same tubular region with intermediate compartment or standing gradient models of isotonic flow (6, 7).

Droplet Limiting Concentration Gradients

Reported values for the Na limiting concentration gradient have decreased over the years, as shown in Table III, which suggests that the original measurements of droplet Na concentration were too low. Our values for the maximum limiting Na concentration gradient, 12 mM with the isotonic raffinose solution and 9 mM with the equilibrium solution, are the smallest that have been reported in mammalian proximal tubules. Furthermore, constant values may not have been attained during our measurements, and the true limiting concentration gradient could be even smaller or nonexistent.

The difference between our values for the limiting gradient and previous reports could be explained by water extraction from our droplets into oil occurring during the manipulation of these small fluid volumes. Indeed, even volumes of nanoliter size will concentrate at room temperature, in spite of being kept under presumably water-saturated oil (30). Therefore, extreme care was taken to use oil freshly saturated with water, to keep the filled micropipettes in a water-saturated atmosphere, to keep fluid droplets exposed to a minimum amount of oil, and to process each sample immediately after collection. As shown in Fig. 2, conservation experiments demonstrate that over a period of several hours there is no significant increase in concentration for 198-pl droplets stored under our conditions; however, there does appear to be a slight initial increase in concentration. This concentrating effect probably occurs during transfer of droplets between volumetric and micropuncture micropipettes, when exposure to a large volume of oil was unavoidable. This increase in concentration is small: 4.4 ± 0.3% (4 experiments, 62 droplets). Because these control experiments involved twice the number of droplet transfers and twice the exposure to a large volume of oil as encountered with standing droplets, the correction should be only ~2%. Such a small correction could not explain the discrepancy with previous reports and has not been applied to the experimental data.

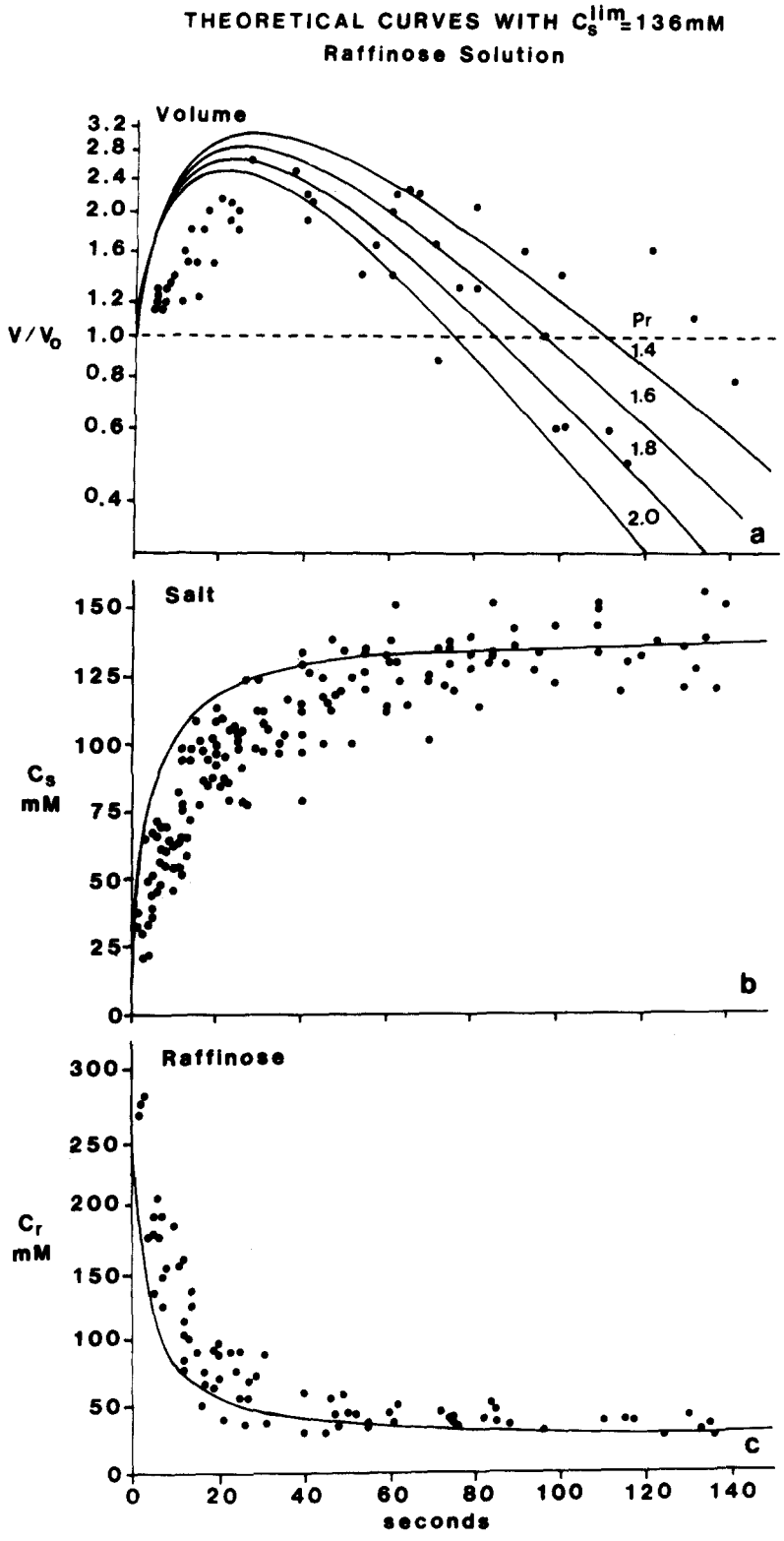
THEORETICAL CURVES WITH C_s^{lim}=136mM
Raffinose Solution
Volume
3.2
2.8
2.4
2.0
1.6
1.2
V/V0
1.0
0.8
0.6
0.4
Pr
1.4
1.6
1.8
2.0
a
Salt
150
125
100
Cs
mM
75
50
25
0
b
Raffinose
300
250
200
Cr
mM
150
100
50
0
c
0
20
40
60
80
100
120
140
seconds

The discrepancy between our observations of higher limiting Na concentrations (or smaller limiting concentration gradients) and previous reports can be explained by the longer exposure times that were used in our studies. Other standing droplet studies have used tubular exposure times of ~60 s or less (22, 24, 25, 32, 35, 39, 62); some studies with solutions resembling our equilibrium solution have used a tubular exposure time of only ~15 s (11, 20). The average values that we obtain with our isotonic raffinose solution evaluated at tubular exposure times between 50 and 70 s (Table II) are 124 ± 3 mM for Na and 125 ± 2 mM for Cl (n = 19); the average value that we obtain for sodium with our equilibrium solution evaluated at tubular exposure time between 10 and 25 s (Table II) is 123 ± 2 mM (n = 34). These values agree well with recently reported limiting concentrations (11, 20, 35, 39). Because our Na concentration values agree with previous determinations when compared over

TABLE III

PREVIOUS DETERMINATIONS OF STANDING DROPLET AND PLASMA Na CONCENTRATIONS AND THE LIMITING CONCENTRATION GRADIENT

Year	Investigator	Droplet	Plasma	ΔC
		mM	*mM*	
1963	Kashgarian et al. (24)	109	155	46
1964	Giebisch et al. (14)	95	144	49
1965	Frick et al. (9)	110	145	35
1965	Hierholzer et al. (22)	109	139	30
1966	Malnic et al. (32)	114	145	31
1968	Wiederholt and Wiederholt (62)	109	142	33
1970	Maude (35)	122	140	18
1970	Morgan et al. (39)	118	142	24
1973	Fromter et al. (11)	136	155	19
1976	Gyory and Lingard (20)	124	146	22

equivalent exposure times, our finding that the Na concentration at longer times is significantly higher (Table II) implies that previous measurements were made before the attainment of constant values.

Because of the scatter in the data of Fig. 4–6, it is not clear whether an invariant Na concentration has been reached by 140 s, particularly in view of the significant concentration increases detailed in Table II. It is possible that no limiting gradient would have been found if longer exposure times could have been used. Establishing the existence of a gradient by the use of longer

FIGURE 8. (*opposite*) Theoretical curves for the isotonic raffinose solution; (*a*) droplet volume obtained from Eq. A11; (*b*) salt concentration obtained from the quotient of Eqs. A9 and A11; (*c*) raffinose concentration obtained from the quotient of Eqs. A10 and A11. The equations assume an attained limiting concentration of 136 mM. Experimental data for droplet volume (Fig. 3*a*), salt (Fig. 4*a*), and raffinose concentration (Fig. 6*a*) are superimposed for comparison. In *a*, the four curves in descending order correspond to values for P_r of 1.4, 1.6, 1.8, and 2.0 × 10^{-5} cm/s. V_0 is the initial droplet volume. In *b* and *c* the four curves are nearly identical and are not resolved.

exposure times is limited by the continuing droplet reabsorption, leading to ultrasmall volumes, and by difficulties in maintaining droplets in place for long periods of time. Problems in statistically distinguishing small differences in concentration between plasma and droplet would contribute to the difficulty. Alternatively, the use of an ideal impermeant solute is not feasible; solutes that can be considered impermeant have very large molecular weights, and the inability to accurately determine droplet water content from measured droplet volume compromises accurate measurement of salt concentrations (11, 49). Experimentally we can only conclude that if a limiting gradient does exist, its magnitude is small, with a maximum value of ~10 mM.

Active Transport Contribution to Volume Reabsorption

If we assume that a limiting gradient is obtained and that the droplet Na concentration that we measured after 100 s represents this limiting value, then we can use the derivation in Appendix A (Eq. A6) to evaluate the active transport rate (K_s). As discussed above, the limiting Na concentration (or limiting salt concentration) may be higher than our measured value. Consequently, as seen from Eq. A5, K_s calculated from our Na concentration measurements will be a maximum value; if a higher limiting Na concentration were chosen, K_s would be smaller, all other parameters being constant. To evaluate K_s from Eq. A6, the following constants were obtained from the literature:

Salt permeability $$P_s = \frac{2P_{Na}P_{Cl}}{P_{Na} + P_{Cl}} = 15.2 \times 10^{-5} \text{ cm/s (26)}$$

$$(P_{Na} = 16.4, P_{Cl} = 14.1 \times 10^{-5} \text{ cm/s [11, 55]}).*$$

Salt reflection coefficient $$\sigma_s = 0.69 \text{ (54, 55)}.$$

Plasma salt concentration $$C'_s = (C'_{Na}C'_{Cl})^{1/2} = 127 \text{ mM (45, 60)}$$

$$(C'_{Na} = 145 \text{ mM}, C'_{Cl} = 112 \text{ mM [cf. Results]}).$$

Systemic plasma values were used for peritubular Na and Cl concentrations. Recent reports have observed differences between peritubular and systemic Cl concentrations, with Cl being 4–7 mM lower in the peritubular plasma (3, 61). The use of a lower peritubular Cl concentration would augment the passive reabsorption force; we have instead chosen to use the more conservative systemic values, thus minimizing the passive movement of salt.

The remaining two constants to be evaluated for Eq. A6, the raffinose permeability (P_r) and raffinose reflection coefficient (σ_r) are not well known. Values for P_r of 1.0×10^{-5} cm/s (13) and 1.07×10^{-5} cm/s (4) have been reported; however, they have been calculated using the standing droplet technique according to a procedure which we have shown potentially underestimates true values (59). We have shown in an example of a nonelectrolyte

* These apparent permeabilities probably include the effect of an electrical potential; because they were measured using a solution similar to our equilibrium solution and the isotonic raffinose solution (after the initial 30 s), their use is appropriate here.

(polyethylene glycol) permeability determination using the standing droplet technique that the true permeability determination would be underestimated by 43% (Fig. 7 of ref. 59). Assuming a similar error in the previous raffinose determinations (4, 13), the corrected (average) raffinose permeability is 1.48 $\times$ 10^{-5} cm/s. For the remaining parameter of Eq. A6, σ_r, we will simply assume a value of 0.9. We will show that the value we obtain for K_s is little affected by our choice for σ_r.

Using the above constants and our measured value for the droplet limiting salt concentration of 136 mM, the maximum value for the active transport rate (K_s) is calculated from Eq. A6 to be 0.085 $\times$ 10^{-5} cm/s. Total droplet volume flow (J_v) after the attainment of limiting gradients is given by Eq. A4. Comparing volume flow due to K_s with total J_v (in equivalent units), active transport accounts for only 5.5% of the volume reabsorption (with σ_r = 0.80, this value becomes 8.9%; with σ_r = 1.0, the value is 2.1%).

The active transport rate has also been evaluated by fitting the experimental data to a theoretical model of the standing droplet solved in closed form (Appendix B). To obtain a closed form solution it was necessary to use an equation that approximates droplet volume. The equation we have chosen (Eq. A8) was obtained by equating the effective osmotic pressure of standing droplet and plasma (Eq. A7). Although effective osmotic pressure equilibrium may not be attained in the proximal tubule, deviations from true equilibrium should be small due to the high hydraulic conductivity of this tissue (2, 55). Similarly, Eq. A7 does not formally apply to our droplet at $t = 0$, but again because of the high hydraulic conductivity of the proximal tubule the osmotic adjustments will probably be rapid and the equation should apply to our experimental points obtained after a few seconds. This is supported by our observations (shown in Fig. 7 and mentioned in Results) that the ideal osmotic pressures of droplet and plasma are already equivalent within experimental error in the earliest samples, and that droplet osmolality does not change with time. Under these conditions the true initial droplet volume will be greater than the injected 200 pl.

In addition to using an approximation for droplet volume, the solution to the equations of Appendix B is itself an approximation in that $\bar{C}_s$ and $\bar{C}_r$ are treated as constant terms in order to obtain a closed form solution. Values for these constants were calculated using the arithmetic mean (26) of the measured plasma and limiting droplet concentration values. This approximation of constant average concentrations will overestimate volume (and salt) influx at early times with droplets of the raffinose solution. Our resulting estimate of the active transport rate will again be a maximum value, since larger theoretical active transport rates will be required to fit the experimental data at later time points.

The theoretical curves represented by Eqs. A9–A11 of Appendix B were evaluated using the previously chosen parameter values for P_s, C'_s, C_s^{lim}, and σ_s. The proximal tubular radius was assumed to be 15 μm (55). Using our measured limiting concentrations and plasma values (Results), $\bar{C}_s$ = 131 mM and $\bar{C}_r$ = 16 mM. We have assumed σ_r = 0.90. Using our measured limiting concentrations and the above reflection coefficients, the effective

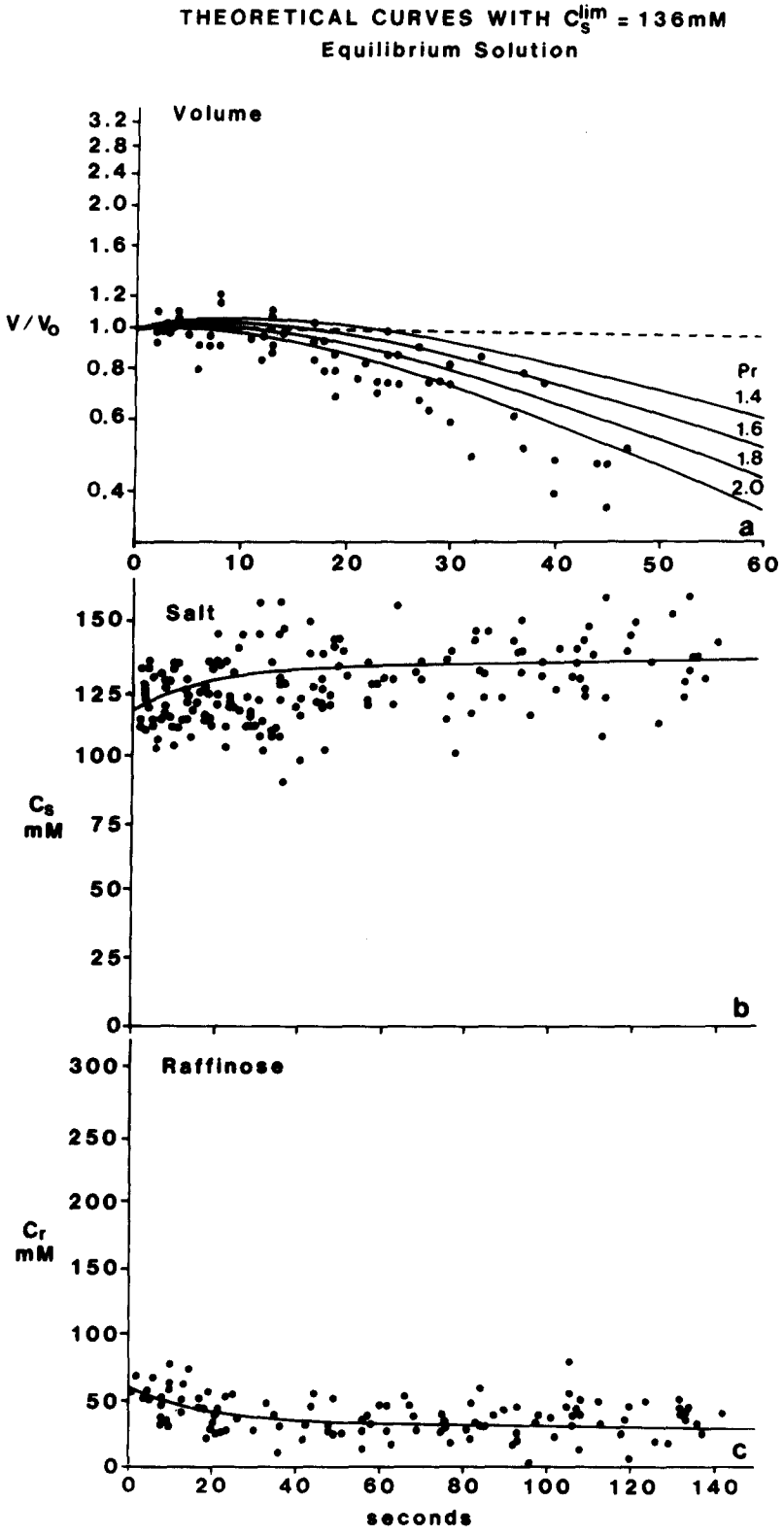
THEORETICAL CURVES WITH C_s^{lim} = 136mM
Equilibrium Solution
Volume
V/Vo
3.2
2.8
2.4
2.0
1.6
1.2
1.0
0.8
0.6
0.4
Pr
1.4
1.6
1.8
2.0
a
0
10
20
30
40
50
60
Salt
Cs
mM
150
125
100
75
50
25
0
b
Raffinose
Cr
mM
300
250
200
150
100
50
0
c
0
20
40
60
80
100
120
140
seconds

osmotic pressure (C_e) calculated from the right side of Eq. 7 is 213 mM. The two constants that remain to be determined, P_r and K_s, are not independent but are linked by Eq. A12. We have varied P_r between the previously measured value of 1.0×10^{-5} cm/s and twice this measured value, 2.0×10^{-5} cm/s. We do not believe the previous measurements could be in error by more than this amount. For each value of P_r the corresponding value for K_s was calculated from Eq. A12. K_s was found to be negative for $P_r < 1.4 \times 10^{-5}$ cm/s. A negative value for K_s would indicate active salt transport into the droplet, contrary to all observations, and consequently we have considered only values for P_r between 1.4 and 2.0×10^{-5} cm/s. Using these values we have evaluated the theoretical Eqs. A9–11 and compared these equations with the experimental data. This comparison is shown in Figs. 8 and 9 for P_r values of 1.4, 1.6, 1.8, and 2.0×10^{-5} cm/s.

Each single theoretical line shown in Figs. 8*b* and *c* and 9*b* and *c* is a juxtaposition of four lines corresponding to the variation of P_r over its allowed range (P_r = 1.4, 1.6, 1.8, and 2.0×10^{-5} cm/s). For the isotonic raffinose solution these values for P_r correspond to active NaCl transport rates (K_s) of 0.03, 0.18, 0.32, and 0.47×10^{-5} cm/s, respectively (Eq. A12). Variation of the coupled values of P_r and K_s over this range has no effect on the graphs, and all curves fit the experimental data for solute concentration. An equivalent fit to the concentration data can be obtained in the absence of an active salt pump (K_s = 0). Consequently, the experimentally observed limiting Na concentration gradient does not necessarily indicate the presence of an active pump since it can be obtained using only passive forces.

As shown in Figs. 8*a* and 9*a*, the droplet volume is affected by the choice of the raffinose permeability (and hence active transport rate), and a clear separation of the curves is obtained. The value of $P_r = 1.5 \times 10^{-5}$ cm/s gives the best nonlinear (nonweighted) least-squares fit to the experimental data of Fig. 8*a* (fitting performed for $t \geq 60$ s; not shown). As can be estimated from Fig. 8*a*, the curve for $P_r = 1.5 \times 10^{-5}$ cm/s would overestimate the experimentally observed volume maximum (as expected due to the use of constant values for $\bar{C}_s$ and $\bar{C}_r$) but predicts well the time at which the volume maximum is obtained. For the equilibrium solution (Fig. 9*a*) the model predicts the initial slow volume decrease observed from the experimental data. Although with the equilibrium solution (Fig. 9*a*) the raffinose permeability of 1.5×10^{-5} cm/s would appear to overestimate the volume, it is likely that the true volume has been experimentally underestimated (31, 52) as previously discussed.

From Eq. A12, $P_r = 1.5 \times 10^{-5}$ cm/s corresponds to an active salt transport rate of 0.10×10^{-5} cm/s, equivalent to a J_v of only 0.06 nl/mm·min

FIGURE 9. (*opposite*) As described in Fig. 8, theoretical curves for the equilibrium solution for droplet volume (*a*), salt concentration (*b*), and raffinose concentration (*c*) with time. Experimental data for droplet volume (Fig. 3*b*), salt (Na, Fig. 5*a*) and raffinose concentration (Fig. 6*b*) are superimposed for comparison. As described in Fig. 8, each graph contains four theoretical curves corresponding to P_r = 1.4, 1.6, 1.8, and 2.0×10^{-5} cm/s.

(calculated as $A \times K_s$ where A is the nephron area exposed to the droplet). From Eq. A11, the limiting value for total J_v is 0.89 nl/min·min, and active salt transport accounts for 6.4% of the volume reabsorption. Again due to our choice of values for $\bar{C}_s$ and $\bar{C}_r$, this contribution of active NaCl transport to volume reabsorption is an overestimation.

It could be argued that the value for total J_v that we are modeling, 0.89 nl/mm·min in the above example, is much reduced from the commonly observed value of 3 nl/mm·min for volume flow in the rat proximal tubule (13), indicating that raffinose has in some manner shut down the Na pump. We would then not be expected to observe a contribution of active Na transport to transepithelial volume flow. Although we cannot disprove this possibility, we would argue against this interpretation for two reasons: (*a*) the ability of a simple molecule-like raffinose to interfere with the Na pump would be novel and we feel highly unlikely; and (*b*) the decrease in volume flow observed in standing droplets can be readily explained by the effect of raffinose on passive forces. As discussed previously (60), under free-flow conditions volume reabsorption due to the passive of solute asymmetry is the result of both salt moving out of the droplet down the chloride gradient and the difference in effective osmotic pressure between droplet and plasma. In the standing droplet, not only is the chloride gradient reduced, but the osmotic pressure of the poorly permeant solute (~30 mM raffinose, Table II) diminishes the difference in effective osmotic pressure between droplet and plasma. This dual change in the passive reabsorptive forces could explain the 70% reduction in volume flow observed in standing droplets.

There is little direct evidence for an important role of an active Na pump in transepithelial fluid movement in the convoluted proximal tubule. The available evidence is largely indirect and subject to additional interpretations; for instance, the recent observation in the colon (53) that an increase in the intracellular Na concentration can diminish the Na conductance of the luminal membrane, if generally applicable, provides an alternative interpretation to the effect of ouabain (34, 50) or low temperature (47) on transcellular Na transport in the proximal tubule. Similarly, the observation that fluid reabsorption occurs in the presence of an osmotic agent such as mannitol (14, 63) (in which the luminal Na concentration is less than that of plasma), need not indicate active Na reabsorption but could be explained by the passive movement of Cl.

The comparison of our experimental measurements with the two different theoretical developments of Appendices A and B indicates that the contribution of active salt transport to volume flow in standing droplets is small: ~6%. Our results do not address the existence of active transport for other solutes that could contribute directly or indirectly to volume reabsorption. Obviously the development of solute asymmetry under free-flow conditions depends on active transport processes. These active epithelial transport processes occur in the early proximal tubule and involve the efflux of solutes other than Na, such as HCO_3, glucose, and amino acids. In the intermediate and late proximal tubule, there is no dissipation of the concentration gradients of these

solutes either because the permeabilities of these solutes are zero, which is unlikely, or because the influx of these solutes down their concentration gradient is constantly opposed by active reabsorption processes. Although the cycle of passive influx and active reabsorption of these solutes would probably not directly contribute to volume reabsorption, indirectly it would maintain the solute asymmetry responsible for passive salt and volume reabsorption from the droplet.

As an alternative to our second theoretical development involving the use of Eq. A8, we have also solved Eqs. A1 and A2 in closed form using an equation for droplet volume obtained by equating the ideal osmotic pressure of droplet and plasma (equations and derivation not shown). This latter approximation for droplet volume has been justified experimentally (Results, Fig. 7, and references 17 and 58). Comparison of the theoretical curves with the experimental data yields results similar to Figs. 8 and 9. The best fit to the experimental isotonic raffinose data gave a value of $P_r = 1.7 \times 10^{-5}$ cm/s corresponding to $K_s = 0.19 \times 10^{-5}$ cm/s. Under these conditions K_s accounts for 11% of the droplet reabsorptive rate.

APPENDIX A

The equations for the movement of salt and raffinose in standing droplets are based on the principles of irreversible thermodynamics (26). Raffinose movement is a result of simple diffusion and solvent drag:

$$\frac{dn_r}{dt} = \frac{d(C_r V)}{dt} = -AP_r C_r + \frac{dV}{dt}(1 - \sigma_r)\bar{C}_r \qquad \text{(A1)}$$

Salt movement contains in addition an active component:

$$\frac{dn_s}{dt} = \frac{d(C_s V)}{dt} = AP_s(C_s - C'_s) - AK_s C_s + \frac{dv}{dt}(1 - \sigma_s)\bar{C}_s \qquad \text{(A2)}$$

In the above equations:

t = time;
n_i = amount of i in the standing droplet, where i stands for either salt (s) or raffinose (r);
V = droplet volume;
A = nephron area exposed to the standing droplet;
P_i = permeability of i;
C_i = concentration of i in the droplet;
C'_s = concentration of salt in the plasma (interstitium);
K_s = active NaCl transport rate in cm/s;
σ_i = reflection coefficient of i for the proximal tubular epithelium; and
$\bar{C}_i$ = average concentration of i across the tubular epithelium.

These equations include the major reabsorptive forces. The following development does not use an explicitly defined volume flow; consequently, all

forces acting on the droplet volume are implicitly included in the above equations.

The above equations for droplet reabsorption assume that the epithelium can be treated as a single homogeneous membrane. This is a common approach (11, 26, 41, 46–49) that is consistent with the use of permeabilities and reflection coefficients that have been measured using this same assumption. The model also assumes that the standing droplet consists only of salt, raffinose, and water, that the raffinose concentration is negligible in the plasma, and that the active transport mechanism is operating well below saturation.

It has been suggested that NaCl transport in the rat proximal tubule is electrically neutral (35). Eq. A2 describes but is not limited to transport of a neutral salt. Eq. A2 can also be applied to ionic fluxes for the simple system we describe as has been theoretically demonstrated (45). Because of the constraint of electroneutrality, for a single (dissociated) salt the net ionic fluxes must be equal regardless of the electrical potential.

When a limiting gradient is obtained $dC_r/dt = 0$, and from Eq. A1 it can be shown (assuming the droplet to be a right circular cylinder) that

$$\frac{dV}{dt} = \frac{4P_rV}{\rho(1 + \sigma_r)} \tag{A3}$$

where ρ is the droplet radius. From Eq. A3 and the assumption that the droplet is a right circular cylinder, volume flow or J_v (defined as $[dV/dt]/A$ [26]) is given by the equation:

$$J_v = \frac{2P_r}{1 + \sigma_r}. \tag{A4}$$

Similarly, with the attainment of a limiting gradient $dC_s/dt = 0$, and combining Eq. A2 with Eq. A3 it can be shown that the limiting concentration gradient (C_s^{lim}) is given by the equation:

$$C_s^{lim} = C_s' \frac{P_s - P_r[(1 - \sigma_s)/(1 + \sigma_r)]}{P_s + K_s - P_r[(1 + \sigma_s)/(1 + \sigma_r)]}. \tag{A5}$$

If $\sigma_r = \sigma_s = 1$, Eq. A4 reduces to that previously published for the limiting gradient in the absence of solvent drag (60).

From Eq. A5, K_s is given by

$$K_s = P_s\left(\frac{C_s' - C_s^{lim}}{C_s^{lim}}\right) + P_r\left[\frac{(1 + \sigma_s)C_s^{lim} - (1 - \sigma_s)C_s'}{(1 + \sigma_r)C_s^{lim}}\right]. \tag{A6}$$

APPENDIX B

The equations for the movement of salt and raffinose in standing droplets are given by Eq. A1 and A2, respectively, of Appendix A. We have approximated droplet volume by equating the effective osmotic pressure of plasma and droplet. The condition for osmotic pressure equilibrium between plasma and

droplet is given by

$$\Sigma_j \sigma_j C_j' = C_e = \sigma_r C_r + 2\sigma_s C_s. \tag{A7}$$

The subscript j denotes a constituent of the plasma. C_e is the effective osmotic pressure of plasma for the proximal tubule. The other symbols have been previously defined in Appendix A. Limitations in the applicability of this equation to our standing droplets are discussed in the text. Solving Eq. A7 for droplet volume gives

$$V = (\sigma_r n_r + 2\sigma_s n_s)/C_e. \tag{A8}$$

Eqs. A1, A2, and A8 can be solved in closed form if the average concentrations $\bar{C}_s$ and $\bar{C}_r$ of Eqs. A1 and A2 are chosen to be constant. The choice of constant average concentrations is discussed in the text. With constant $\bar{C}_s$ and $\bar{C}_r$, the solution to Eqs. A1, A2, and A8 is as follows:

$$n_s = ae^{M_1 t} + be^{M_2 t} \tag{A9}$$

$$n_r = ce^{M_1 t} + de^{M_2 t} \tag{A10}$$

and

$$V = (2\sigma_s a + \sigma_r c)e^{M_1 t} + (2\sigma_s b + \sigma_r d)e^{M_2 t} \tag{A11}$$

where

$$a = \frac{(M_2 - 2E)n_{s,0} - Fn_{r,0}}{M_2 - M_1}, \quad b = \frac{Fn_{r,0} - n_{s,0}(M_1 - 2E)}{M_2 - M_1}$$

$$c = \frac{[(M_2 - 2E)n_{s,0} - Fn_{r,0}](M_1 - 2E)}{(M_2 - M_1)F},$$

$$d = \frac{(M_2 - 2E)[Fn_{r,0} - n_{s,0}(M_1 - 2E)]}{(M_2 - M_1)F}$$

where $n_{s,0}$ and $n_{r,0}$ equal the amount of salt or raffinose, respectively, in the standing droplet at $t = 0$, and

$$E = \frac{(2P_s C_s' \sigma_s - P_s C_e - K_s C_e)(C_e - \sigma_r(1 - \sigma_r)\bar{C}_r)}{\rho C_e(C_e - \sigma_r(1 - \sigma_r)\bar{C}_r - 2\sigma_s(1 - \sigma_s)\bar{C}_s)}$$

$$F = \frac{2P_s C_s' \sigma_r(C_e - \sigma_r(1 - \sigma_r)\bar{C}_r) - 2\sigma_r(1 - \sigma_s)\bar{C}_s P_r C_e}{\rho C_e(C_e - \sigma_r)(1 - \sigma_r)\bar{C}_r - 2\sigma_s(1 - \sigma_s)\bar{C}_s)}$$

$$M_1 = E + G + [(E + G)^2 + 4(FH - EG)]^{1/2}$$

$$M_2 = E + G - [(E + G)^2 + 4(FH - EG)]^{1/2}$$

$$G = \frac{\sigma_s(1 - \sigma_r)\bar{C}_r F - P_r C_e}{\rho(C_e - \sigma_r(1 - \sigma_r)\bar{C}_r)}$$

and

$$H = \frac{\sigma_s(1 - \sigma_r)\bar{C}_r E}{(C_e - \sigma_r(1 - \sigma_r)\bar{C}_r)}.$$

The remaining parameters are defined in Appendix A.

The equation for the salt limiting concentration is evaluated as before (60) by taking the ratio of Eqs. A9 and A11, dividing numerator and denominator by the slower exponent, and taking the limit at large time. For the isotonic raffinose droplet it can be shown that

$$C_s^{\lim} = \frac{FC_e}{\sigma_r(M_1 - 2E) + 2F\sigma_s}. \tag{A12}$$

In addition to the assumptions that droplets are at osmotic equilibrium with plasma and that the average concentrations are constant, the derived equations assume that the concentration of raffinose is negligible in the plasma, that solutes in the plasma other than Na and Cl are effectively impermeant (which may include the participation of active reabsorption of these non-NaCl solutes, thus maintaining low droplet concentrations), that the droplet can be approximated by a right circular cylinder containing only Na, Cl, and raffinose, and that the active NaCl pump is operating well below saturation.

We thank one of the reviewers for suggesting the derivation used in Appendix A.
This research was supported by grants RR-PO-RR00679 and NIAMDD-R01-AM16898 from the National Institutes of Health. A portion of this work was completed at Procter and Gamble Co., Miami Valley Laboratories, Cincinnati, Ohio 45247.

Received for publication 23 March 1979 and in revised form 22 September 1981.

REFERENCES

1. ABRAHAM, E. H., R. R. WARNER, and C. P. LECHENE. 1975. Electron probe analysis of the effect of parathyroid hormone on inorganic ions in the rat kidney. Proc. 10th Ann. Conf. Microbeam Analysis Soc., Las Vegas, Nevada. 47A–47F.
2. ANDREOLI, T. E., J. A. SCHAFER, and S. L. TROUTMAN. 1978. Perfusion rate-dependence of transepithelial osmosis in isolated proximal convoluted tubules: estimation of the hydraulic conductance. *Kid. Int.* **14**:263–269.
3. ATHERTON, J. C. 1977. Comparison of chloride concentration and osmolality in proximal tubular fluid, peritubular capillary plasma and systemic plasma in the rat. *J. Physiol. (Lond.)*. **273**:765–773.
4. BERRY, C. A., and F. C. RECTOR, JR. 1977. Hydraulic water conductivity of junctional complexes in rat proximal convoluted tubule. 10th Ann. Meeting Am. Soc. Nephrology, Washington, D.C. 99A.
5. BURG, M. B., and N. GREEN. 1976. Role of monovalent ions in the reabsorption of fluid by isolated perfused proximal renal tubules of the rabbit. *Kid. Int.* **10**:221–228.
6. CURRAN, P. F., and J. R. MCINTOSH. 1962. A model system for biological water transport. *Nature (Lond.)*. **193**:347–348.
7. DIAMOND, J. M., and W. H. BOSSERT. 1967. Standing gradient osmotic flow: a mechanism for coupling of water and solute transport in epithelia. *J. Gen. Physiol.* **50**:2061–2083.
8. EARLEY, L. E., and R. W. SCHRIER. 1973. Intrarenal control of sodium excretion by hemodynamic and physical factors. *In* Handbook of Physiology. Renal Physiology. J. Orloff and R. W. Berliner, editors. Am. Physiol. Soc., Washington, D.C. 721–762.

9. FRICK, A., G. RUMRICH, K. J. ULLRICH, and W. E. LASSITER. 1965. Microperfusion study of calcium transport in the proximal tubule of the rat kidney. *Pflugers Archiv.* **286:**109–117.
10. FROHNERT, P. P., B. HOHMANN, R. ZWIEBEL, and K. BAUMANN. 1970. Free flow micropuncture studies of glucose transport in the rat nephron. *Pflugers Archiv.* **315:**66–85.
11. FROMTER, E., G. RUMRICH, and K. J. ULLRICH. 1973. Phenomenologic description of Na^+, Cl^- and HCO_3^- absorption from proximal tubules of the rat kidney. *Pflugers Archiv.* **343:**189–220.
12. FROMTER, E., and K. GESSNER. 1974. Free-flow potential profile along rat kidney proximal tubule. *Pflugers Archiv.* **351:**69–83.
13. GERTZ, K. H. 1963. Transtubulare natriumchloridflusse und permeabilitat fur nichtelektrolyte im proximalen und distalen konvolut der rattenniere. *Pflugers Archiv.* **276:**336–356.
14. GIEBISCH, G., R. M. KLOSE, G. MALNIC, W. J. SULLIVAN, and E. E. WINDHAGER. 1964. Sodium movement across single perfused proximal tubules of rat kidneys. *J. Gen. Physiol.* **47:**1175–1194.
15. GIEBISCH, G., and E. E. WINDHAGER. 1964. Renal tubular transfer of sodium, chloride and potassium. *Am. J. Med.* **36:**643–669.
16. GIEBISCH, G., and E. E. WINDHAGER. 1973. Electrolyte transport across renal tubular membranes. *In* Handbook of Physiology. Renal Physiology. J. Orloff and R. W. Berliner, editors. Am. Physiol. Soc., Washington, D.C. 315–376.
17. GOTTSCHALK, C. W., and M. MYLLE. 1959. Micropuncture study of the mammalian urinary concentrating mechanism: evidence for the countercurrent hypothesis. *Am. J. Physiol.* **196:**927–936.
18. GOTTSCHALK, C. W., and W. E. LASSITER. 1973. Micropuncture methodology. *In* Handbook of Physiology. Renal Physiology. J. Orloff and R. W. Berliner, editors. Am. Physiol. Soc., Washington, D.C. 129–143.
19. GYORY, A. Z. 1971. Reexamination of the split oil droplet method as applied to kidney tubules. *Pflugers Arch.* **324:**328–343.
20. GYORY, A. Z., and J. M. LINGARD. 1976. Kinetics of active sodium transport in rat proximal tubules and its variation by cardiac glycosides at zero net volume and ion fluxes. Evidence for a multisite sodium transport system. *J. Physiol. (Lond.).* **257:**257–274.
21. HAMBURGER, R. J., N. L. LAWSON, and J. H. SCHWARTZ. 1976. Response to parathyroid hormone in defined segments of proximal tubule. *Am. J. Physiol.* **230:**286–290.
22. HIERHOLZER, K., M. WIEDERHOLT, H. HOLZGREVE, G. GIEBISCH, R. M. KLOSE, and E. E. WINDHAGER. 1965. Micropuncture study of renal transtubular concentration gradients of sodium and potassium in adrenalectomized rats. *Pflugers Archiv.* **285:**193–210.
23. JACOBSON, H. R., and D. W. SELDIN. 1977. Proximal tubular reabsorption and its regulation. *Annu. Rev. Pharmacol. Toxicol.* **17:**623–646.
24. KASHGARIAN, M., H. STOCKLE, C. W. GOTTSCHALK, and K. J. ULLRICH. 1963. Transtubular electrochemical potentials of sodium and chloride in proximal and distal renal tubules of rats during antidiuresis and water diuresis (*Diabetes insipidus*). *Pflugers Archiv.* **227:**89–106.
25. KASHGARIAN, M., Y. WARREN, and H. LEVITIN. 1965. Micropuncture study of proximal renal tubular chloride transport during hypercapnea in the rat. *Am. J. Physiol.* **209:**655–658.
26. KATCHALSKY, A., and P. F. CURRAN. 1967. Nonequilibrium Thermodynamics in Biophysics. Harvard University Press, Cambridge, Mass. 113–148.

27. LECHENE, C., F. MOREL, M. GUINNEBAULT, and C. DEROUFFIGNAC. 1969. Etude par microponction de l'elaboration de l'urine. *Nephron.* **6**:457–477.

28. LECHENE, C. 1970. The use of the electron microprobe to analyze very minute amounts of liquid samples. Proc. Fifth Nat. Conf. on Electron Probe Analysis, New York. 32A–32C.

29. LECHENE, C. 1974. Electron probe microanalysis of picoliter liquid samples. *In* Microprobe Analysis as Applied to Cells and Tissues. T. Hall, P. Echlin, and R. Kaufmann, editors. Academic Press, Inc., New York. 351–367.

30. LECHENE, C., and R. WARNER. 1979. Electron probe analysis of liquid droplets. *In* Microbeam Analysis in Biology. C. Lechene and R. Warner, editors. Academic Press, Inc., New York. 279–297.

31. LEGRIMELLEC, C., P. POUJEOL, and D. G. SHIRLEY. 1975. A note on the split-droplet technique as applied to proximal tubules of the rat kidney. *J. Physiol. (Lond.).* **249**:45–46.

32. MALNIC, G., R. M. KLOSE, and G. GIEBISCH. 1966. Microperfusion study of distal tubular potassium and sodium transfer in rat kidney. *Am. J. Physiol.* **211**:548–559.

33. MARSH, D. J., K. J. ULLRICH, and G. RUMRICH. 1963. Micropuncture analysis of the behavior of potassium ions in rat renal cortical tubules. *Pflugers Archiv.* **227**:107–119.

34. MAUDE, D. L. 1969. Effects of K and ouabain on fluid transport and cell Na in proximal tubule in vitro. *Am. J. Physiol.* **216**:1199–1206.

35. MAUDE, D. L. 1970. Mechanism of salt transport and some permeability properties of rat proximal tubule. *Am. J. Physiol.* **216**:1590–1595.

36. MAUNSBACH, A. B. 1973. Ultrastructure of the proximal tubule. *In* Handbook of Physiology. Renal Physiology. J. Orloff and R. W. Berliner, editors. Am. Physiol. Soc., Washington, D.C. 31–79.

37. MOHER, T., and C. LECHENE. 1975. Automated electron probe analysis of biological samples. *Biosci. Commun.* **1**:314–329.

38. MOREL, F., and Y. MURAYAMA. 1970. Simultaneous measurement of unidirectional and net sodium fluxes in microperfused rat proximal tubules. *Pflugers Archiv.* **320**:1–23.

39. MORGAN, T., M. TADAKORO, D. MARTIN, and R. W. BERLINER. 1970. Effect of furosemide on Na^+ and K^+ transport studied by microperfusion of the rat nephron. *Am. J. Physiol.* **218**:292–297.

40. NAKAJIMA, K., J. R. CLAPP, and R. R. ROBINSON. 1970. Limitations of the shrinking-drop micropuncture technique. *Am. J. Physiol.* **219**:345–357.

41. NEUMANN, K. H., and F. C. RECTOR, JR. 1976. Mechanism of NaCl and water reabsorption in the proximal convoluted tubule of rat kidney. *J. Clin. Invest.* **58**:1110–1118.

42. PERSSON, A. E. G., B. AGERUP, and J. SCHNERMANN. 1972. The effect of luminal application of colloids on rat proximal tubular net fluid flux. *Kid. Int.* **2**:203–213.

43. RAMSAY, J. A., and R. H. J. BROWN. 1955. Simplified apparatus and procedures for freeze-point determinations upon small volumes of fluid. *J. Sci. Instruments.* **32**:372–375.

44. RECTOR, F. C., M. MARTINEZ-MALDONADO, F. P. BRUNNER, and D. W. SELDIN. 1966. Evidence for passive reabsorption of NaCl in proximal tubule of rat kidney. *J. Clin. Invest.* **45**:1060.

45. RICHARDSON, I. W. 1971. Ionic flows through a single homogeneous membrane. *J. Membr. Biol.* **4**:3–15.

46. RICHARDSON, I. W., V. LICKO, and E. BARTOLI. 1974. Mechanisms of salt and water transport in proximal tubule as measured by split drop. *J. Theor. Biol.* **47**:57–64.

47. SCHAFER, J. A., C. S. PATLAK, and T. E. ANDREOLI. 1975. A component of fluid absorption linked to passive ion flows in the superficial pars recta. *J. Gen. Physiol.* **66**:445–471.

48. SCHAFER, J. A., C. S. PATLAK, and T. E. ANDREOLI. 1977. Fluid absorption and active and passive ion flows in the rabbit superficial pars recta. *Am. J. Physiol.* **233:**F154–167.

49. SCHAFER, J. A., C. S. PATLAK, S. L. TROUTMAN, and T. E. ANDREOLI. 1978. Volume absorption in the pars recta. II. Hydraulic conductivity coefficient. *Am. J. Physiol.* **234:**F340–F348.

50. SCHATZMANN, H. J., E. E. WINDHAGER, and A. K. SOLOMON. 1958. Single proximal tubules of the *Necturus* kidney. II. Effect of 2,4-dinitrophenol and ouabain on water reabsorption. *Am. J. Physiol.* **195:**570–574.

51. SEELY, J. F., and E. CHIRITO. 1975. Studies of the electrical potential difference in rat proximal tubule. *Am. J. Physiol.* **229:**72–80.

52. SHIRLEY, D. G., P. POUJEOL, and C. LEGRIMELLEC. 1976. Phosphate, calcium and magnesium fluxes into the lumen of the rat proximal convoluted tubule. *Pflugers Archiv.* **362:**247–254.

53. TURNHEIM, K., R. A. FRIZZEL, and S. G. SCHULTZ. 1977. Effect of anions on amiloride-sensitive, active sodium transport across rabbit colon, in vitro. *J. Membr. Biol.* **37:**63–84.

54. ULLRICH, K. J., G. RUMRICH, and B. SCHMIDT-NIELSEN. 1967. Reflection coefficient of different nonelectrolytes in the proximal convolution of the rat kidney. *Fed. proc.* **26:**375.

55. ULLRICH, K. J. 1973. Permeability characteristics of the mammalian nephron. *In* Handbook of Physiology. Renal Physiology. J. Orloff and R. W. Berliner, editors. Am. Physiol. Soc., Washington, D.C. 377–398.

56. ULLRICH, K. J., G. RUMRICH, and S. KLOSS. 1976. Active Ca^{2+} reabsorption in the proximal tubule of the rat kidney. *Pflugers Archiv.* **364:**223–228.

57. VILLEY, D., and T. ANAGNOSTOPOULOS. 1973. Sodium-free fluid reabsorption in *Necturus* kidney perfused with sodium-free media. *Kid. Int.* **4:**252–258.

58. WALKER, A. M., P. A. BOTT, J. OLIVER, and M. C. MACDOWELL. 1941. The collection and analysis of fluid from single nephrons of the mammalian kidney. *Am. J. Physiol.* **134:**580–595.

59. WARNER, R. R., and C. P. LECHENE. 1979. Analysis of proximal tubule salt and water transport in standing droplets. *J. Theor. Biol.* **77:**453–471.

60. WARNER, R. R., and C. P. LECHENE. 1980. Isosmotic volume reabsorption in rat proximal tubule. *J. Gen. Physiol.* **76:**559–586.

61. WEINSTEIN, S. W., and J. SZYJEWICZ. 1976. Early postglomerular plasma concentrations of chloride, sodium and inulin in the rat kidney. *Am. J. Physiol.* **231:**822–831.

62. WEIDERHOLT, M., and B. WIEDERHOLT. 1968. Der einfluss von dexamethason auf die wasser- und elektrolytausscheidung adrenalektomierter ratten. *Pflugers Archiv.* **302:**57–78.

63. WINDHAGER, E. E., and G. GIEBISCH. 1961. Micropuncture study of renal tubular transfer of sodium chloride in the rat. *Am. J. Physiol.* **200:**581–590.

64. WINDHAGER, E. E. 1974. Mechanisms of reabsorption and excretion of ions and water. *In* Physiology of the Kidney and Body Fluids. R. F. Pitts, editor. Year Book Med. Publishers, Chicago. 99–139.

65. WINDHAGER, E. E., and G. GIEBISCH. 1976. Proximal sodium and fluid transport. *Kid. Int.* **9:**121–133.